American Mineralogist, Volume 80, pages 21–26, 1995

Crystal chemistry of the monazite and xenotime structures

YUNXIANG NI, JOHN M. HUGHES
Department of Geology, Miami University, Oxford, Ohio 45056, U.S.A.
ANTHONY N. MARIANO
48 Page Brook Road, Carlisle, Massachusetts 01741, U.S.A.

ABSTRACT

Monazite and xenotime, the $RE(PO_4)$ dimorphs, are the most ubiquitous rare earth (RE) minerals, yet accurate structure studies of the natural phases have not been reported. Here we report the results of high-precision structure studies of both the natural phases and the synthetic $RE(PO_4)$ phases for all individual stable rare earth elements.

Monazite is monoclinic, $P2_1/n$, and xenotime is isostructural with zircon (space group $I4_1/amd$). Both atomic arrangements are based on [001] chains of intervening phosphate tetrahedra and RE polyhedra, with a REO_8 polyhedron in xenotime that accommodates the heavy lanthanides (Tb–Lu in the synthetic phases) and a REO_9 polyhedron in monazite that preferentially incorporates the larger light rare earth elements (La–Gd). As the structure "transforms" from xenotime to monazite, the crystallographic properties are comparable along the [001] chains, with structural adjustments to the different sizes of RE atoms occurring principally in (001).

There are distinct similarities between the structures that are evident when their atomic arrangements are projected down [001]. In that projection, the chains exist in (100) planes, with two planes per unit cell. In monazite the planes are offset by 2.2 Å along [010], relative to those in xenotime, in order to accommodate the larger light RE atoms. The shift of the planes in monazite allows the RE atom in that phase to bond to an additional O2′ atom to complete the REO_9 polyhedron.

INTRODUCTION AND PREVIOUS WORK

The rare earth (RE; here considered as lanthanides + Y) phosphates, $RE(PO_4)$, exist in nature as the phases monazite and xenotime; monazite preferentially incorporates the larger, light rare earth elements (LREEs, here La–Gd) whereas xenotime tends to incorporate the smaller, heavy rare earth elements (HREEs, here Tb–Lu, + Y). The phases are important accessory minerals in granitoids and rhyolites, and, because of their incorporation of rare earth elements (REEs) and high distribution coefficients of REEs, they can effectively control REE distribution in igneous rocks despite the fact that they usually occur only as an accessory phase. A review of the composition and geological occurrence of monazite in the accessory mineral assemblage of granitoids was given by Rapp and Watson (1986).

Despite the fact that monazite is the most common REE-bearing mineral and both RE phosphates are ubiquitous ore minerals of the REEs, the atomic arrangements of the natural phases are not well characterized. The most recent structure studies of natural monazite were reported by Ueda (1967) and Ghouse (1968). The former study, undertaken using film data for *h0l* (55) and *hk*0 (58) reflections, refined to *R* values of 16 and 19%, respectively, for the two sets of planes, and yielded impossibly large P-O distances. The work by Ghouse (1968) detailed the common problem of metamictization and demonstrated that structural changes are induced upon annealing of the phase. The results of his film study are incompatible with the Ueda (1967) study and yield tetrahedral P-O bond lengths as long as 1.69 Å, certainly unreasonable. The crystal structure of natural xenotime is poorly characterized as well. The most recent study reported an *R* value of 10% (Krstanovic, 1965), on the basis of 38 film-derived intensities, and P-O bond distances that are unreasonably short.

Because of the crystal-chemical similarity between the lanthanide elements and actinide elements, monazite has been investigated for use as a solid-state repository for radioactive waste (see, e.g., Boatner and Sales, 1988). A portion of this evaluative work has involved refining the crystal structures of all synthetic $RE(PO_4)$ phases save $Pm(PO_4)$ (Mullica et al., 1985a, 1985b, 1984; Milligan et al., 1982, 1983a, 1983b; Beall et al., 1981). However, the variation of several parameters derived from the crystal structure refinements is discontinuous when plotted vs. atomic number, and electron density residua of the refinements were >4 e/Å^3 for several of the structures. There is a clear need to obtain a complete set of high-precision structure refinements for the complete series of $RE(PO_4)$ phases (save Pm). The following reports the results of those studies and the first high-precision structure refine-

0003–004X/95/0102–0021$02.00

TABLE 1. Crystal data and results of structure refinements for monazite structure phases

Phases	Monazite*	La(PO_4)	Ce(PO_4)	Pr(PO_4)	Nd(PO_4)	Sm(PO_4)	Eu(PO_4)	Gd(PO_4)
				Unit cells by least squares (unconstrained)				
a (Å)	6.7902(10)	6.8313(10)	6.7880(10)	6.7596(8)	6.7352(10)	6.6818(12)	6.6613(10)	6.6435(9)
b (Å)	7.0203(6)	7.0705(9)	7.0163(8)	6.9812(10)	6.9500(9)	6.8877(9)	6.8618(9)	6.8414(10)
c (Å)	6.4674(7)	6.5034(9)	6.4650(7)	6.4344(9)	6.4049(8)	6.3653(9)	6.3491(8)	6.3281(6)
α (°)	90.007(8)	89.993(11)	89.997(9)	89.997(11)	90.004(10)	89.982(11)	90.005(11)	90.013(9)
β (°)	103.38(1)	103.27(1)	103.43(1)	103.53(1)	103.68(1)	103.86(1)	103.96(1)	103.976(9)
γ (°)	89.989(9)	89.981(11)	90.011(10)	89.979(10)	89.967(11)	89.979(12)	89.975(12)	89.983(11)
No. collected	3541	1945	1910	1884	1860	1812	1797	1778
No. unique	945	891	943	861	851	827	819	811
No. > $3\sigma_I$	774	790	717	753	763	732	712	710
R_{merge}	0.012	0.014	0.011	0.012	0.010	0.013	0.012	0.011
R	0.015	0.017	0.014	0.016	0.015	0.016	0.016	0.016
R_w	0.023	0.026	0.019	0.021	0.017	0.019	0.019	0.019
				Largest peaks on difference maps (e/Å³)				
(+)	0.741	0.897	0.653	0.971	0.841	0.885	1.039	1.073
(−)	0.704	1.023	0.632	1.276	0.995	1.236	0.884	1.265
				Atomic positions				
RE x	0.28152(4)	0.28154(2)	0.28182(2)	0.28177(2)	0.28178(3)	0.28153(3)	0.28152(3)	0.28150(3)
y	0.15929(4)	0.16033(2)	0.15914(2)	0.15862(3)	0.15806(3)	0.15638(3)	0.15595(3)	0.15529(3)
z	0.10006(4)	0.10068(2)	0.10008(2)	0.09988(2)	0.09950(3)	0.09813(3)	0.09757(3)	0.09695(3)
B (Å²)	0.329(4)	0.294(3)	0.431(3)	0.351(3)	0.280(3)	0.228(3)	0.193(3)	0.306(3)
P x	0.3048(2)	0.3047(1)	0.3047(1)	0.3040(1)	0.3037(1)	0.3034(2)	0.3029(1)	0.3031(2)
y	0.1630(2)	0.1639(1)	0.1635(1)	0.1630(1)	0.1626(1)	0.1618(2)	0.1615(1)	0.1612(2)
z	0.6121(2)	0.6121(1)	0.6124(1)	0.6127(1)	0.6127(1)	0.6130(2)	0.6130(1)	0.6131(2)
B (Å²)	0.31(2)	0.33(1)	0.51(1)	0.36(1)	0.30(1)	0.25(2)	0.24(1)	0.38(2)
O1 x	0.2501(5)	0.2503(4)	0.2508(4)	0.2498(4)	0.2502(4)	0.2499(5)	0.2513(4)	0.2539(5)
y	0.0068(5)	0.0077(4)	0.0055(4)	0.0051(4)	0.0046(4)	0.0020(5)	0.0012(4)	0.0013(5)
z	0.4450(5)	0.4477(4)	0.4458(4)	0.4441(4)	0.4430(4)	0.4405(5)	0.4409(4)	0.4385(5)
B (Å²)	0.63(6)	0.78(4)	0.93(4)	0.69(4)	0.67(5)	0.57(6)	0.68(5)	0.80(6)
O2 x	0.3814(5)	0.3799(4)	0.3811(4)	0.3816(4)	0.3815(4)	0.3822(5)	0.3833(4)	0.3837(5)
y	0.3307(6)	0.3315(3)	0.3320(3)	0.3327(4)	0.3331(4)	0.3341(5)	0.3350(4)	0.3346(5)
z	0.4975(6)	0.4964(4)	0.4982(4)	0.4990(4)	0.4987(4)	0.5008(5)	0.5017(4)	0.5024(5)
B (Å²)	0.69(6)	0.61(4)	0.80(4)	0.67(4)	0.61(4)	0.57(5)	0.52(5)	0.66(5)
O3 x	0.4742(6)	0.4748(4)	0.4745(4)	0.4744(4)	0.4747(4)	0.4748(5)	0.4743(4)	0.4729(5)
y	0.1070(6)	0.1071(4)	0.1054(4)	0.1046(4)	0.1040(4)	0.1025(5)	0.1022(4)	0.1016(5)
z	0.8037(6)	0.8018(4)	0.8042(4)	0.8057(4)	0.8073(4)	0.8102(5)	0.8116(4)	0.8126(5)
B (Å²)	0.73(6)	0.63(4)	0.84(4)	0.63(4)	0.62(5)	0.56(5)	0.53(5)	0.62(5)
O4 x	0.1274(5)	0.1277(3)	0.1268(3)	0.1260(4)	0.1249(4)	0.1217(5)	0.1204(4)	0.1187(5)
y	0.2153(5)	0.2168(3)	0.2164(4)	0.2150(4)	0.2153(4)	0.2125(5)	0.2135(4)	0.2138(5)
z	0.7104(6)	0.7101(4)	0.7108(4)	0.7120(4)	0.7127(4)	0.7113(5)	0.7119(5)	0.7131(5)
B (Å²)	0.63(6)	0.66(4)	0.77(4)	0.62(4)	0.52(4)	0.57(5)	0.48(4)	0.67(5)

* Natural sample.

ments of natural monazite and xenotime and elucidates the relationship between the two structures.

EXPERIMENTAL METHODS

The crystals of 14 synthetic RE(PO_4) phases were obtained from L. Boatner of Oak Ridge National Laboratory. The synthesis methods are described in the structure studies cited above. The specimen of natural monazite-(Ce) is a euhedral, optical-quality crystal from the Kangankunde carbonatite, Malawi. By wet chemical analysis of the REEs, its formula is $(Ce_{0.51}La_{0.29}Nd_{0.14}Pr_{0.05}Sm_{0.01})_{\Sigma 1.00}(PO_4)$. The natural xenotime-(Y) sample is from the Nanling granitoid, southeast China. It is a euhedral, optical-quality crystal; electron microprobe analysis of the crystal gave $(Y_{0.77}Dy_{0.07}Er_{0.05}Yb_{0.03}Gd_{0.02}Ho_{0.02}Ca_{0.01})_{\Sigma 0.97}(P_{1.01}Si_{0.01})_{\Sigma 1.02}O_4$. The atomic arrangements of natural monazite-(Ce) and xenotime-(Y) ultimately were refined to $R = 0.015$ and 0.016, respectively, in part attesting to the quality of the crystals. To obviate absorption effects, small crystals (0.07–0.16 mm) were used in data collection.

X-ray intensity data were collected using a CAD4 automated diffractometer, with graphite-monochromated Mo$K\alpha$ radiation. Unit-cell dimensions were determined by least-squares refinement of 25 automatically centered reflections and are given in Tables 1 and 2. The axial dimensions vary systematically with Z_{RE}, as noted in Figure 1. The unit-cell dimensions are predictable from the equations noted in that figure, which also allows prediction of the mean radius of the RE occupant of the RE(PO_4) phase from the unit-cell dimensions. The equations were derived from the data obtained from the synthetic crystals, and the predicted mean radius of the RE occupant of the natural phases and mean radius as calculated from the chemical analysis are in good agreement. It can be noted that the unit cell of Tb(PO_4) xenotime is larger than that of Gd(PO_4) monazite, despite the fact that Tb^{3+} is smaller than Gd^{3+}, demonstrating a more closely packed O array in monazite than in xenotime.

Data were collected in a θ-2θ mode to 60° 2θ, except for Lu(PO_4) (to 64°); a hemisphere of data was collected for all the samples except natural monazite, for which a

TABLE 2. Crystal data and results of structure refinements for xenotime structure phases

Phases	Xenotime*	$Tb(PO_4)$	$Dy(PO_4)$	$Ho(PO_4)$	$Er(PO_4)$	$Tm(PO_4)$	$Yb(PO_4)$	$Lu(PO_4)$
Unit cells by least squares (unconstrained)								
a (Å)	6.8951(6)	6.9319(12)	6.9046(12)	6.8772(8)	6.8510(13)	6.8297(7)	6.8083(9)	6.7848(14)
b (Å)	6.8943(5)	6.9299(11)	6.9057(9)	6.8773(12)	6.8505(16)	6.8290(10)	6.8103(6)	6.7807(10)
c (Å)	6.0276(6)	6.0606(11)	6.0384(6)	6.0176(8)	5.9968(10)	5.9798(10)	5.9639(5)	5.9467(6)
α (°)	89.993(7)	90.016(14)	90.013(9)	90.004(13)	89.986(16)	90.009(12)	89.987(7)	89.969(10)
β (°)	90.012(8)	89.997(14)	90.019(12)	89.991(10)	89.963(14)	89.967(11)	89.997(9)	90.008(12)
γ (°)	90.018(7)	89.997(13)	90.006(13)	89.988(13)	90.026(17)	89.996(10)	90.019(9)	90.010(14)
No. collected	919	924	922	903	891	884	890	1046
No. unique	145	135	134	132	130	129	128	151
No. > $3\sigma_I$	109	113	112	111	108	107	97	119
R_{merge}	0.018	0.010	0.011	0.014	0.014	0.020	0.013	0.016
R	0.016	0.009	0.008	0.015	0.012	0.017	0.013	0.009
R_w	0.028	0.019	0.019	0.021	0.022	0.026	0.033	0.012
Largest peaks on difference maps (e/Å³)								
(+)	0.624	0.464	0.496	0.669	1.105	0.934	0.817	0.978
(−)	0.766	0.498	0.537	1.283	0.922	1.187	0.734	0.802
Atomic positions								
RE x	0	0	0	0	0	0	0	0
y	0.75	0.75	0.75	0.75	0.75	0.75	0.75	0.75
z	0.125	0.125	0.125	0.125	0.125	0.125	0.125	0.125
B (Å²)	0.455(7)	0.350(4)	0.346(4)	0.049(6)	0.406(7)	0.104(7)	0.28(1)	0.245(2)
P x	0	0	0	0	0	0	0	0
y	0.25	0.25	0.25	0.25	0.25	0.25	0.25	0.25
z	0.375	0.375	0.375	0.375	0.375	0.375	0.375	0.375
B (Å²)	0.62(2)	0.43(2)	0.43(2)	0.26(4)	0.48(4)	0.14(4)	0.50(7)	0.31(2)
O x	0	0	0	0	0	0	0	0
y	0.0753(6)	0.0764(5)	0.0760(6)	0.0757(8)	0.0743(9)	0.072(1)	0.074(1)	0.0735(4)
z	0.2158(6)	0.2175(5)	0.2162(6)	0.2165(8)	0.216(1)	0.213(1)	0.215(1)	0.2138(4)
B (Å²)	0.94(6)	0.60(5)	0.61(5)	0.38(8)	0.65(9)	0.3(1)	0.5(1)	0.52(4)

* Natural sample.

full sphere was collected. Other experimental conditions are listed in Tables 1 and 2. Data reduction and refinement procedures are as given in Ni et al. (1993). Atomic positions for the monazite samples are listed in Table 1 and for the xenotime samples in Table 2. Table 3 contains selected bond distances for natural monazite-(Ce), synthetic $Ce(PO_4)$, natural xenotime-(Y), and synthetic $Ho(PO_4)$. Table 4 contains anisotropic displacement parameters for all atoms in the structures, and Table 5 contains calculated and observed structure factors for all the samples.[1]

DISCUSSION OF THE ATOMIC ARRANGEMENTS

Monazite has the space group $P2_1/n$, and xenotime, a zircon isostructure, $I4_1/amd$. Both structures have equal numbers of PO_4 tetrahedra and REO_x polyhedra. Monazite incorporates the larger light lanthanides in a REO_9 polyhedron, whereas xenotime possesses a more regular REO_8 polyhedron that accommodates the smaller HRE elements, both structures reflecting the most common coordination number for the respective groups of REE (Miyawaki and Nakai, 1987). The tetrahedra in both structure types are isolated, separated by intervening REO_x polyhedra; O atoms in each structure coordinate to two RE and one P atoms. The fundamental atomic arrangements of monazite and xenotime are given in the aforementioned papers on the structures of the synthetic phases, which describe the structures as [001] chains formed of alternating RE polyhedra and phosphate tetrahedra (so-called polyhedron-tetrahedron chains). We expand on that

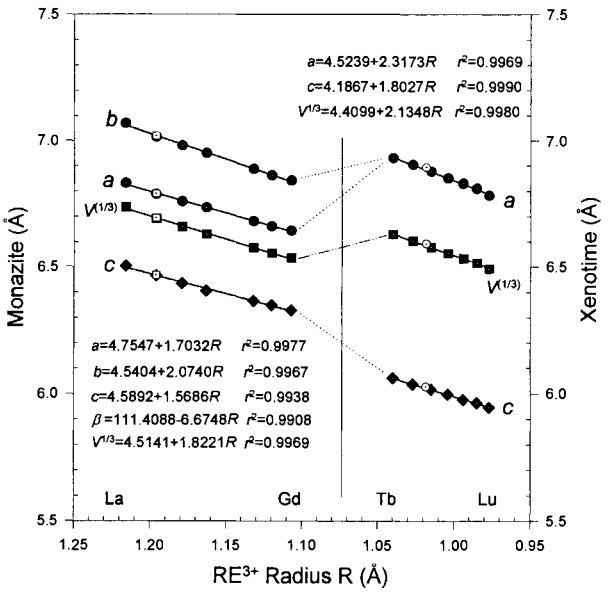

Fig. 1. Variation of lattice parameters with RE element for synthetic $RE(PO_4)$ phases. RE radius from Shannon (1976). Open symbols denote natural phases analyzed in this study.

[1] Tables 4 and 5 may be ordered as Document AM-95-578 from the Business Office, Mineralogical Society of America, 1130 Seventeenth Street NW, Suite 330, Washington, DC 20036, U.S.A. Please remit $5.00 in advance for the microfiche.

TABLE 3. Selected interatomic distances (Å) for natural and synthetic monazite and xenotime

Atoms	Distance	Atoms	Distance
Natural monazite-(Ce)		**Ce(PO$_4$)**	
RE-O1	2.528(2)	Ce-O1	2.535(2)
O1′	2.461(2)	O1′	2.452(3)
O2	2.776(3)	O2	2.783(2)
O2′	2.644(2)	O2′	2.646(2)
O2″	2.573(2)	O2″	2.563(2)
O3	2.585(3)	O3	2.584(3)
O3′	2.481(2)	O3′	2.468(2)
O4	2.526(2)	O4	2.524(2)
O4′	2.455(2)	O4′	2.446(2)
Mean	2.559	Mean	2.556
P-O1	1.524(3)	P-O1	1.530(3)
O2	1.545(3)	O2	1.546(3)
O3	1.534(3)	O3	1.539(2)
O4	1.531(3)	O4	1.535(3)
Mean	1.534	Mean	1.538
O1-O2	2.437(4)	O1-O2	2.451(4)
O3-O4	2.414(4)	O3-O4	2.425(3)
O1′-O2′	3.403(6)	O1′-O2′	3.400(4)
O2′-O2″	2.867(6)	O2′-O2″	2.854(3)
O2″-O3′	2.793(5)	O2″-O3′	2.788(3)
O3′-O4′	2.831(6)	O3′-O4′	2.811(4)
O4′-O1′	2.970(6)	O4′-O1′	2.969(3)
Natural xenotime-(Y)		**Ho(PO$_4$)**	
Y-O × 4	2.382(4)	Ho-O × 4	2.379(5)
O′ × 4	2.309(4)	O′ × 4	2.307(5)
Mean	2.346	Mean	2.343
P-O × 4	1.540(4)	P-O × 4	1.532(5)
O-O	2.409(7)	O-O	2.397(8)
O-O′	2.801(7)	O-O′	2.806(7)
O-O′	2.958(7)	O-O′	2.953(6)
O′-O′	3.355(8)	O′-O′	3.354(6)

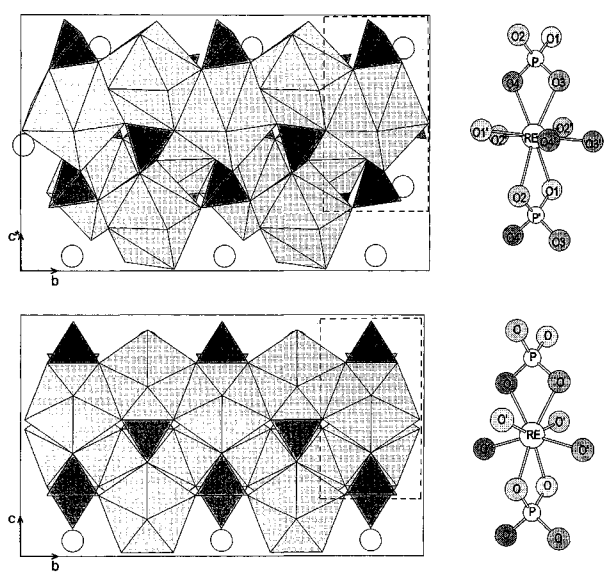

Fig. 2. Atomic arrangements of monazite (**top**) and xenotime (**bottom**). Polyhedral projections down [100] illustrate the similarity between the two atomic arrangements. Ball and stick chains and atomic nomenclature for each structure are depicted to right; ball and stick depictions are rotated about **c*** for clarity of viewing. Dashed line outlines polyhedron-tetrahedron chain illustrated on right. Open circles represent RE atoms.

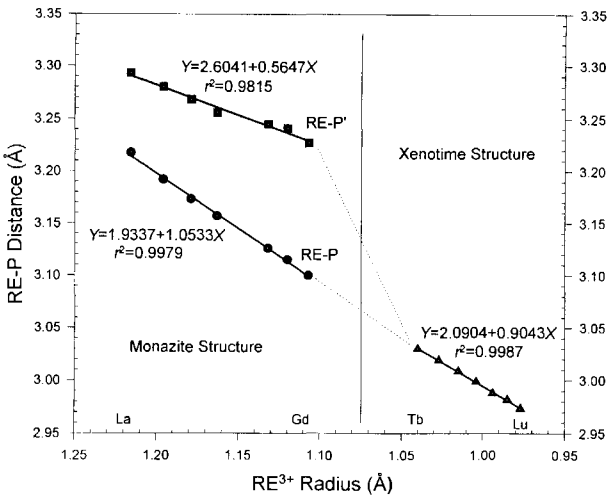

Fig. 3. RE-P distance in polyhedron-tetrahedron chains in synthetic monazite and xenotime phases. RE radius from Shannon (1976).

description here and offer the relationship between the chains in the two phases.

Figure 2 depicts the polyhedron-tetrahedron chains in the two RE(PO$_4$) structures. The chains differ principally in the coordination of the RE component of the chain, with HREO$_8$ coordination in the xenotime chain and LREO$_9$ polyhedron in the monazite chain. The chains extend along [001] by sharing tetrahedral edges with RE polyhedra; there are four chains per unit cell in each mineral. The chains are linked laterally [in (001)] by sharing edges of adjacent REO$_x$ polyhedra (Fig. 2). As the structural aspects of both monazite and xenotime can be represented by these polyhedron-tetrahedron chains, discussion of the crystal-chemical details of the phases can focus

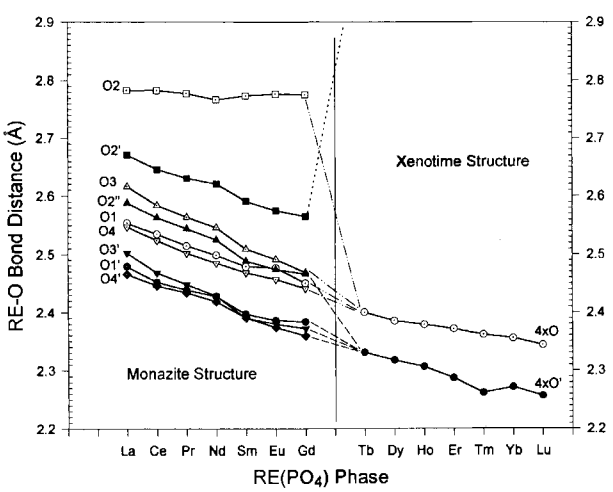

Fig. 4. Selected RE-O bond distances in synthetic RE(PO$_4$) phases.

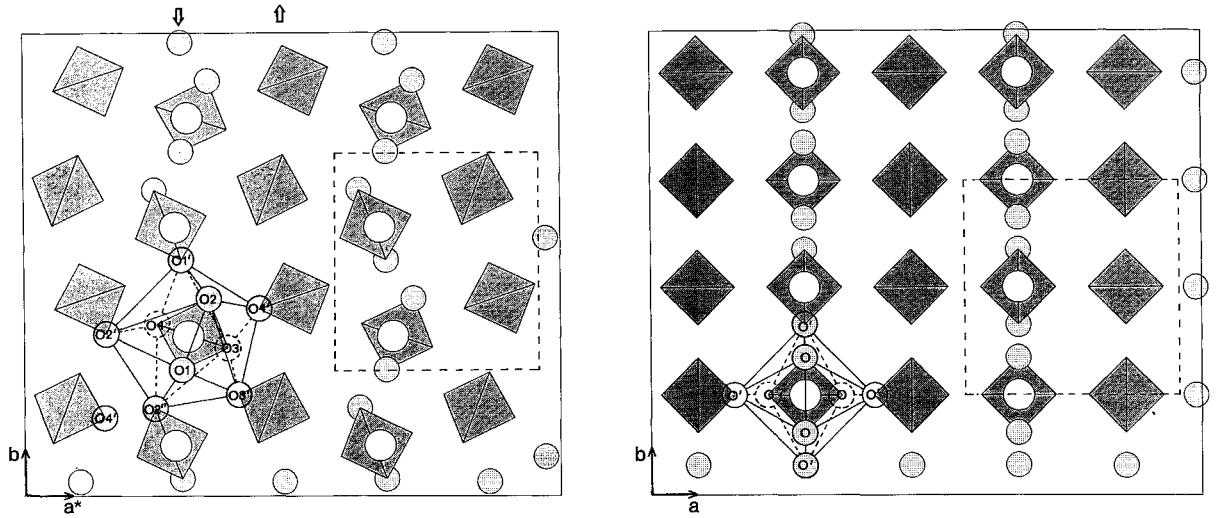

Fig. 5. Comparison of monazite and xenotime phases projected down [001], with unit cells outlined by dashed line. The diagrams illustrate the changes in RE-O bonds that occur during the "transition" between the monazite and xenotime phases. The arrows in the left diagram depict the direction of shifts in (100) planes of phosphate tetrahedra required to relate the monazite phosphate planes to those in xenotime. Larger open circles represent RE atoms; smaller circles represent O atoms.

on the regular changes in properties of the polyhedron and tetrahedron with Z_{RE}.

As expected, intrachain RE-P distances vary regularly with Z_{RE}. In the monazite structure, two distinct RE-P distances (RE-P, RE-P′) exist along the chain, as compared with one in the xenotime structure. Figure 3 depicts the variation of RE-P distances with the radius of REE. The shorter RE-P distances in the monazite polyhedron-tetrahedron chain and the RE-P distance in the xenotime polyhedron-tetrahedron chain vary linearly with RE radius, with a slope close to 1. The cation-cation distances are extremely short for trivalent and pentavalent cations; for example, in several of the xenotime structures the P-REE distance is <3 Å, and yet REE-O bond distances of >3 Å are commonly reported. The cation-cation repulsion that results from this close approach is mitigated by short O-O distances on the intervening tetrahedral edge. These O-O distances are as short as 2.39 Å and exhibit a general decrease with decreasing radius of the RE substituent. That these RE-P distances are a function of RE radius and are independent of structure type suggests that crystallographic properties along [001] are similar for both structure types and validates the [001] polyhedron-tetrahedron chain comparison of the atomic arrangements.

Xenotime has two (× 4) unique RE-O bond distances, whereas monazite has nine unique RE-O bond distances. Regular variation of these RE-O distances occurs with Z_{RE} in the two structures; Figure 4 illustrates the RE-O bond distances in the synthetic $RE(PO_4)$ phases. As will be detailed below, the RE polyhedra in the two structures are similar; the RE cation in monazite bonds to an O2′ atom that is extra relative to xenotime as a result of the incorporation of the larger LREE.

Monazite-xenotime structural relationships

The structural relationships between monazite and xenotime have not been previously elucidated. The relationship between the atomic arrangements is clearly evident, however, in the juxtaposition of [001] projections of the two structures. As illustrated in Figure 5, the phosphate tetrahedra in both structures exist in planes perpendicular to **a***, with two such planes in the unit cell of each phase; each of these tetrahedra represents the projection of a polyhedron-tetrahedron chain. In monazite, the tetrahedra in adjacent (100) planes are offset from each other principally along [010], and O-O edges of the tetrahedra are inclined to the crystallographic axes; in xenotime, the tetrahedra are in rows parallel to **a** and **b**, and the shared edges of the tetahedron are parallel to **a** or **b**. The structures are related by these shifts of the (100) planes (2.23 Å along [010] and $\frac{1}{2}a \cos \beta = 0.79$ Å along [001], as shown in Fig. 5) and a slight rotation of the tetrahedron about [001].

Given the similarities of the crystal-chemical properties of the REEs save for ionic radius, the existence of two $RE(PO_4)$ structures must result to a large extent from the incorporation of REEs of different sizes. In xenotime, the atomic arrangement accommodates the smaller HREE in the REO_8 polyhedron, the most common coordination for the HREE (Miyawaki and Nakai, 1987). However, Tb is the largest REE that the structure accommodates; to incorporate larger RE elements, a "transition" occurs that creates a larger REO_9 polyhedron, the most common coordination for the LREE (Miyawaki and Nakai, 1987). The "transition" occurs by the shift of the neighboring (100) planes, as explained above.

As illustrated in Figure 5, the change in coordination of the RE polyhedron from the xenotime to monazite atomic arrangements is accomplished by breaking a RE-O4′ bond and adding RE-O2′ and RE-O4′ bonds. At the monazite-xenotime compositional boundary (between Gd and Tb) the xenotime TbO_8 polyhedron has a smaller volume than the monazite GdO_9 polyhedron (23.7 Å^3 vs. 29.4 Å^3, with four RE polyhedra in each unit cell). The molar volume of xenotime-(Tb), however, is larger than that of monazite-(Gd) (291 Å^3 vs. 279 Å^3) despite the fact that xenotime-(Tb) incorporates the smaller REE. The void space in xenotime-(Tb) is thus substantially larger than that in monazite-(Gd), creating an energetically unfavorable situation with exceptionally short and long O-O nearest neighbor distances (the importance of void space in the structures has also been suggested by Taylor and Ewing, 1978, in their study of the monazite and xenotime isostructures, huttonite and thorite.) Because of the inflexibility in both structures of the RE-O-P sequence in the [001] polyhedron-tetrahedron chains, the additional RE-O bond in monazite is added in the void space in the (001) equatorial plane of the RE polyhedron, thus removing the [001] tetrad and accommodating the larger LREEs in monazite.

Acknowledgments

Funding for this work was provided by the National Science Foundation through grant EAR-9218577. Harold D. Rowe participated in early parts of the project as a portion of his senior thesis research, and L. Arnold Miller of Molycorp, Inc., provided the analysis of natural monazite. L.A. Boatner of ORNL kindly provided the synthetic $RE(PO_4)$ phases to A.N.M., and Shimei Yu provided the sample of natural xenotime. The manuscript was improved by reviews by Daniel E. Appleman and T. Scott Ercit; Scott Ercit provided particularly insightful comments on the transition between the monazite and xenotime structures.

References cited

Beall, G.W., Boatner, L.A., Mullica, D.F., and Milligan, W.O. (1981) The structure of cerium orthophosphate, a synthetic analogue of monazite. Journal of Inorganic Nuclear Chemistry, 43, 101–105.

Boatner, L.A., and Sales, B.C. (1988) Monazite. In W. Lutze and R.C. Ewing, Eds., Radioactive waste forms for the future, p. 495–564. Elsevier Science, Amsterdam.

Ghouse, K.M. (1968) Refinement of the crystal structure of heat-treated monazite crystal. Indian Journal of Pure and Applied Physics, 6, 265–268.

Krstanovic, I. (1965) Redetermination of oxygen parameters in xenotime, YPO_4. Zeitschrift für Kristallographie, 121, 315–316.

Milligan, W.O., Mullica, D.F., Beall, G.W., and Boatner, L.A. (1982) Structural investigations of YPO_4, $ScPO_4$, and $LuPO_4$. Inorganica Chimica Acta, 60, 39–43.

——— (1983a) The structures of three lanthanide orthophosphates. Inorganica Chimica Acta, 70, 133–136.

——— (1983b) Structures of $ErPO_4$, $TmPO_4$, and $YbPO_4$. Acta Crystallographica, C39, 23–24.

Miyawaki, R., and Nakai, I. (1987) Crystal structures of rare earth minerals. Rare Earths (Kidorui), 11, 1–133.

Mullica, D.F., Milligan, W.O., Grossie, D.A., Beall, G.W., and Boatner, L.A. (1984) Ninefold coordination in $LaPO_4$: Pentagonal interpenetrating tetrahedral polyhedron. Inorganica Chimica Acta, 95, 231–236.

Mullica, D.F., Grossie, D.A., and Boatner, L.A. (1985a) Structural refinements of praseodymium and neodymium orthophosphate. Journal of Solid State Chemistry, 58, 71–77.

——— (1985b) Coordination geometry and structural determinations of $SmPO_4$, $EuPO_4$, and $GdPO_4$. Inorganica Chimica Acta, 109, 105–110.

Ni, Y., Hughes, J.M., and Mariano, A.N. (1983) The atomic arrangement of bastnäsite-(Ce), $Ce(CO_3)F$, and structural elements of synchysite-(Ce), röntgenite-(Ce), and parisite-(Ce). American Mineralogist, 78, 415–418.

Rapp, R.P., and Watson, E.B. (1986) Monazite solubility and dissolution kinetics: Implications for the thorium and light rare earth chemistry of felsic magmas. Contributions to Mineralogy and Petrology, 94, 304–316.

Shannon, R.D. (1976) Revised effective ionic radii and systematic studies of interatomic distances in halides and chalcogenides. Acta Crystallographica, A32, 751–767.

Taylor, M., and Ewing, R.C. (1978) The crystal structures of the $ThSiO_4$ polymorphs: Huttonite and thorite. Acta Crystallographica, B34, 1074–1079.

Ueda, T. (1967) Re-examination of the crystal structure of monazite. Journal of the Japanese Association of Mineralogists, Petrologists, and Economic Geologists, 58, 170–179.

Manuscript received March 28, 1994
Manuscript accepted September 20, 1994